Linear triazole-linked pseudo oligogalactosides as scaffolds for galectin inhibitor development

Christophe Dussouy, Chandan Kishor, Annie Lambert, Clément Lamoureux, Helen Blanchard, Cyrille Grandjean

▶ **To cite this version:**

Christophe Dussouy, Chandan Kishor, Annie Lambert, Clément Lamoureux, Helen Blanchard, et al.. Linear triazole-linked pseudo oligogalactosides as scaffolds for galectin inhibitor development. Chemical Biology and Drug Design, 2020, 10.1111/cbdd.13683 . hal-02990603

HAL Id: hal-02990603
https://hal.science/hal-02990603v1

Submitted on 5 Nov 2020

HAL is a multi-disciplinary open access archive for the deposit and dissemination of scientific research documents, whether they are published or not. The documents may come from teaching and research institutions in France or abroad, or from public or private research centers.

L'archive ouverte pluridisciplinaire **HAL**, est destinée au dépôt et à la diffusion de documents scientifiques de niveau recherche, publiés ou non, émanant des établissements d'enseignement et de recherche français ou étrangers, des laboratoires publics ou privés.

Linear triazole-linked *pseudo* oligogalactosides as scaffolds for galectin inhibitor development

Running title: Novel scaffold for galectin inhibitors

Christophe Dussouy,[†,1] Chandan Kishor,[†,2] Annie Lambert,[1] Clément Lamoureux,[1] Helen Blanchard,[2,3,*] and Cyrille Grandjean[1,*]

[1] Université de Nantes, CNRS, Unité Fonctionnalité et Ingénierie des Protéines (UFIP), UMR 6286, F-44000 Nantes, France

[2] Institute for Glycomics, Griffith University, Gold Coast campus, Queensland 4222, Australia

[3] School of Chemistry & Molecular Bioscience and Molecular Horizons Research Institute, University of Wollongong, Wollongong, NSW 2522, Australia

[†] These authors made equal contributions, joint 1st-authorship.

Correspondence

*Cyrille Grandjean, Unité Fonctionnalité et Ingénierie des Protéines (UFIP), UMR CNRS 6286, Université des Sciences et Techniques de Nantes, 2 rue de la Houssinière, BP92208, 44322 Nantes, France

E.mail: cyrille.grandjean@univ-nantes.fr

*Helen Blanchard, School of Chemistry & Molecular Bioscience and Molecular Horizons Research Institute, University of Wollongong, Wollongong, NSW 2522, Australia

E.mail: helen_blanchard@uow.edu.au

ACKNOWLEDGEMENTS

C.G. gratefully acknowledges the financial support from La Ligue contre le Cancer (Comités de Loire-Atlantique, du Maine et Loire et de Vendée) and the Laboratoires Servier for a post-doctoral fellowship to CD. H.B gratefully acknowledges the financial support from the Cancer council Queensland (Grant ID180845). The MX1 beamline scientists at the Australian Synchrotron, Victoria, Australia are acknowledged for their support during X- ray diffraction data collection.

Funding information

La Ligue contre le Cancer (Comités de Loire-Atlantique, du Maine et Loire et de Vendée) Laboratoires Servier for a post-doctoral fellowship to CD. Cancer Council Queensland grant (Grant ID1080845) awarded to HB.

Abstract

Galectins play key roles in numerous biological processes. Their mode of action depends on their localization which can be extracellular, cytoplasmic or nuclear, and is partly mediated through interactions with β-galactose containing glycans. Galectins have emerged as novel therapeutic targets notably for the treatment of inflammatory disorders and cancers. This has stimulated the design of carbohydrate-based inhibitors targeting the carbohydrate recognition domains (CRDs) of the galectins. Pursuing this approach, we reasoned that linear oligo-galactosides obtained by straightforward iterative click-chemistry could mimic poly-lactosamine motifs expressed at eukaryote cell surfaces which the extracellular form of galectin-3, a prominent member of the galectin family, specifically recognizes. Affinities towards galectin-3 consistently increased with the length of the representative oligogalactosides but without reaching that of oligo-lactosamines. Elucidation of the X-ray crystal structures of the galectin-3 CRD in complex with a synthesized di- and tri-galactoside confirmed that the compounds bind within the carbohydrate-binding site. The atomic structures revealed that binding interactions mainly occur with the galactose moiety at the non-reducing end, primarily with subsites C and D of the CRD, differing from oligo-lactosamine which bind more consistently across the whole groove formed by the five subsites (A-E) of the galectin-3 CRD.

Keywords: galectin-3 inhibitor, galectin, X-ray crystallography, oligogalactosides, 1,2,3-triazole, carbohydrate mimetics

1 | INTRODUCTION

Galectins are an ancient family of proteins found in protozoa through to mammals. In mammals, they are produced as early as embryogenesis and later contribute to homeostasis.(Barondes, 1994),(Johannes, 2018) They are involved in many pathologies including chronic inflammatory diseases as well as cancers.(Sciacchitano, 2018),(Toscano, 2018),(Dubé-Delarosbil, 2018) Hence, galectins are identified as potential therapeutic targets. Galectins are soluble proteins which can be located intra- or extracellularly. They are composed of either one or two carbohydrate recognition domains (CRDs). Galectin-3 is distinct from other family members

as it possesses an N-terminal collagen-like domain in addition to a single CRD.(Barondes, 1994) Their biological activities can involve protein/protein interactions but often imply the binding of glycans that are expressed on glycoproteins to galectin CRDs. This latter feature has been exploited to develop small carbohydrate-based molecules as inhibitors of the most comprehensively studied galectin, the galectin-3. Hence both type I and type II lactosamine(Fort, 2006),(van Hattum, 2013),(Dion, 2017) and thio-digalactose as well as more recently galactose have been successfully used as scaffolds.(Delaine, 2016),(Zetterberg, 2018) The galectin-3 CRD has classically been divided into five subsites (A-E). For these inhibitors, galactose occupies subsite C, stacking against an essential tryptophan (W181 in galectin-3), while galactose aglycons or substituents provide further stabilizing interactions with adjacent subsites.(Oberg, 2011) A major achievement has been the design of bis-{3-deoxy-3-[4-(3-fluorophenyl)-1H-1,2,3-triazol-1-yl]-β-d-galactopyranosyl}sulfane (generally referred to as TD139) that has shown promise for the treatment of idiopathic pulmonary disease.(Delaine et al., 2016) However, these inhibitors are not entirely specific for the galectin-3. We thus sought to exploit the unique propensity of galectin-3 to bind to poly-N-acetyllactosamine, unlike other galectins, with the exception of the galectin-9, to achieve higher selectivity.(Knibbs, 1993),(Hirabayashi, 2002) Structural analyses revealed that galectin-3, galectin-9 N as well as galectin-8 N (albeit at a much lower extent) CRDs can bind not only to terminal, but also to internal *N*-acetyllactosamine units,(Nagae, 2009),(Collins, 2014),(Leffler, 1986) whereas recognition by other members seems to be limited to the terminal Galβ1-4GlcNAc epitope presumably due to steric clashes within the binding site domains.(Bian, 2011) This distinct mode of binding largely accounts for the consistent increase of affinity for both galectin-3 and galectin-9 with increasing length of the N-acetyllactosamine chains. Access to oligo-N-acetyllactosamines has been democratized by the sequential use of glycosyl transferases namely β1,3 or β1,4-galactosyltransferases and β1,3-N-acetylglucosaminyltransferases.(Sauerzapf, 2009),(Fischöder, 2017) We elected to develop *N*-acetyllactosamine oligomer mimics whereby the GlcNAc residues are replaced by triazole units. This could be envisaged through a cost effective and straightforward strategy relying on the preparation of three synthons (two for termination and one for elongation chain) and their iterative assembly using alkyne-azide copper-catalyzed cycloaddition reaction (click-chemistry). Here we report the synthesis of a small set of representative derivatives as well as the determination of their binding affinity towards the galectin-3 CRD in comparison with the N-acetyllactosamine dimer (LN2) and trimer (LN3) as positive controls, using fluorescence polarization. While enhanced affinities

were observed compared to galactose, the affinities of these novel derivatives did not reach that of LN2 or LN3. This prompted us to determine the crystal structures of a di- and a tri-galactoside in complex with the galectin-3 CRD to reveal their mode of binding. These structures establish that the key role in binding is played by the galactose located at the non-reducing end. In addition, the structural results provide insights for modifications of these molecules to further increase their interactions with galectin-3.

2 | MATERIAL AND MATERIALS

2.1 | Material & and general methods

All reagents were purchased from commercial sources and used without further purification. Reactions were monitored by thin-layer chromatography (TLC) on 0.25 mm silica gel plates with fluorescent indicator (GF254) and visualized under UV light. Detection was further achieved by charring with vanillin in sulfuric acid/ethanol (1.5:95 v/v). Flash-chromatography purifications were made on silica gel columns (4 to 80g, 240-400 mesh) using an automated Reveleris Flash Chromatography System (Grace Alltech) equipped by both ELS (Evaporative Light Scattering) and UV/diode array allowing the simultaneous use of two customizable wavelengths detectors.

All NMR experiments were performed at 400.13 MHz using a Bruker Avance 400 MHz spectrometer equipped with a DUAL+ $^{1}H/^{13}C$ ATMA grad 5 mm probe. Assignments were performed by stepwise identification using COSY, and HSQC experiments using standard pulse programs from the Bruker library. Chemical shifts are given relative to external TMS with calibration involving the residual solvent signals. High-resolution mass spectra were recorded in positive mode on Waters SYNAPT G2-Si HDMS with detection with a hybrid quadripole time of flight (Q-TOF) detector. The compounds were individually dissolved in MeOH at a concentration of 1 $mg.mL^{-1}$ and then infused into the electrospray ion source at a flow rate of 10 $\mu L.min^{-1}$ at 100 °C. The mass spectrometer was operated at 3 kV whilst scanning the magnet at a typical range of 4000-100 Da. The mass spectra were collected as continuum profile data. Accurate mass measurement was achieved based on every five second auto-calibration using leucine-enkephalin ($[M+H]^+$ = 556.2771 *m/z*) as internal standard.

2.2 | Experimental procedures for the synthesis of compounds 4-8

Methyl 3-*O*-[1-(β-D-galactopyranosyl)-1,2,3-triazol-4-yl]-methyl-β-D-galactopyranoside 4

To a solution of 1-azido-1-deoxy-β-D-galactopyranose **1** (19.45 mg, 0.095 mmol) in H_2O (265 µL), successive addition of compound **2** (22 mg, 0.095 mmol), *o*-phenylenediamine (40 µL of

a 375 mM aqueous solution), sodium ascorbate (40 µL of a 125 mM aqueous solution) and copper sulfate (40 µL of a 125 mM aqueous solution), was done under argon. The reaction mixture was then stirred under darkness at RT for 2 h. Charcoal was then added and the reaction mixture further stirred at RT overnight, filtered over a Celite pad, concentrated under reduced pressure and further purified under RP-HLPC conditions to give **4** (31 mg, 76%). TLC R_f = 0.34 (AcOEt/*i*PrOH/H_2O 3:2:1); ^{1}H NMR (400 MHz, CD_3OD) δ 8.27 (1 H, s, H triazole), 5.59 (1 H, d, *J* = 9.2 Hz, H-1'), 4.86 (1 H, d, *J* = 12.1 Hz, C*H*H), 4.78 (1 H, d, *J* = 12.1 Hz, CH*H*), 4.18 (1 H, d, *J* = 7.6 Hz, H-1), 4.17 (1 H, t, *J* = 9.2 Hz, H-2'), 4.10 (1 H, br d, *J* = 3.0 Hz, H-4), 4.00 (1 H, br d, *J* = 3.2 Hz, H-4'), 3.86 (1 H, br t, *J* = 5.9 Hz, H-5), 3.83-3.73 (4 H, m, 2 H-6, 2 H-6'), 3.72 (1 H, dd, *J* = 3.2 and 9.2 Hz, H-3'), 3.62 (1 H, dd, *J* = 7.6 and 9.5 Hz, H-2), 3.55 (3 H, s, CH_3), 3.53 (1 H, br t, *J* = 6.5 Hz, H-5'), 3.43 (1 H, dd, *J* = 3.0 and 9.5 Hz, H-3) ; ^{13}C NMR (100 MHz, CD_3OD) δ 145.0 (C alkene), 122.5 (C alkene), 104.4 (C1), 88.8 (C-1'), 81.4 (C-3), 78.5 (C-5), 75.0 (C-5'), 73.9 (C-3'), 70.2 and 70.1 (C-2 and C-2'), 69.0 (C-4'), 65.4 (C-4), 62.1 (CH_2), 61.1 and 61.0 (C-6 and C-6'), 55.9 (CH_3); HR-ESI-MS *m/z* calculated for $C_{16}H_{27}N_3O_{11}$ $(M+Na)^+$ 460.1543, found 460.1561.

Methyl 3-*O*-[1-(3-*O*-propargyl-β-D-galactopyranosyl)-1,2,3-triazol-4-yl]-methyl-β-D-galactopyranoside 5

To a solution of **3** (34.2 mg, 0.11 mmol) in H_2O/tBuOH (1:1) (632 µL), successive addition of **2** (50 mg, 0.21 mmol), *o*-phenylenediamine (40 µL of a 375 mM aqueous solution), sodium ascorbate (40 µL of a 125 mM aqueous solution) and copper sulfate (40 µL of a 125 mM aqueous solution), was done under argon. The reaction mixture was then stirred under darkness at RT for 20 h. The reaction mixture was then concentrated under reduced pressure and the crude residue purified by flash-chromatography on silica gel (eluent: CH_2Cl_2/MeOH 100:0 to CH_2Cl_2/MeOH 70:30) to give compound **5** (28.4 mg, 47%); TLC R_f = 0.24 (CH_2Cl_2/MeOH 8:2); ^{1}H NMR (400 MHz, CD_3OD) δ 8.25 (1 H, s, H triazole), 5.64 (1 H, d, *J* = 9.7 Hz, H-1'), 4.87 (1 H, d, *J* = 12.5 Hz, C*H*H), 4.79 (1 H, d, *J* = 12.5 Hz, CH*H*), 4.48 (dd, 1 H, *J* = 2.44 and 16.1 Hz, C*H*H), 4.42 (dd, 1 H, *J* = 2.44 and 16.1 Hz, C*H*H), 4.28 (1 H, t, *J* = 9.3 Hz, H-2'), 4.24 (1 H, br d, *J* = 3.1 Hz, H-4), 4.19 (1 H, d, *J* = 7.9 Hz, H-1), 4.10 (1 H, br d, *J* = 3.1 Hz, H-4'), 3.87 (1 H, br t, *J* = 6.2 Hz, H-5), 3.83-3.76 (4 H, m, 2 H-6, 2 H-6'), 3.76 (1 H, dd, *J* = 3.2 and 9.2 Hz, H-3'), 3.64 (1 H, dd, *J* = 7.9 and 9.8 Hz, H-2), 3.55 (3 H, s, CH_3), 3.52 (1 H, br t, *J* = 6.2 Hz, H-5'), 3.43 (1 H, dd, *J* = 3.2 and 9.5 Hz, H-3), 2.91 (1 H, t, J = 2.4 Hz, H alkyne); ^{13}C NMR (100 MHz, CD_3OD) δ 145.0 (C alkene), 122.4 (C alkene), 104.4 (C1), 88.7 (C-1'), 81.5 (C-3), 80.7 (C-3'), 79.4 (C alkyne), 78.3 (C-5), 75.0 and 74.9 (C-5' and C alkyne), 70.2 (C-2),

69.1 (C-2'), 66.0 (C-4), 65.5 (C-4'), 62.1 (CH_2), 61.1 and 60.9 (C-6 and C-6'), 56.8 (C alkyne), 55.9 (CH_3); HR-ESI-MS *m/z* calculated for $C_{19}H_{29}N_3O_{11}$ $(M+Na)^+$ 498.1700, found 498.1699.

Methyl 3-*O*-(1-{3-*O*-[1-(β-D-galactopyranosyl)-1,2,3-triazol-4-yl]-methyl-β-D-galactopyranosyl}-1,2,3-triazol-4-yl)-methyl-β-D-galactopyranoside 6

To a solution of **1** (10.6 mg, 51.2 µmol) in H_2O/tBuOH (1:1) (200 µL), successive addition of **5** (16.8 mg, 51.2 µmol), *o*-phenylenediamine (142 µL of a 375 mM aqueous solution), sodium ascorbate (142 µL of a 125 mM aqueous solution) and copper sulfate (142 µL of a 125 mM aqueous solution), was undertaken under argon. The reaction mixture was then stirred under darkness at RT overnight. The reaction mixture was concentrated under reduced pressure and further purified by RP-HPLC (separation was performed on a Uptisphere Strategy 100 Å C18HQ (Interchim, France) (5 µm, 21.2 × 250 mm) column at a flow rate of 6 mL min^{-1} with ELSD and UV (225 nm) detection. Gradient: 0% B for 5 min, 0–50% B over 35 min; Solvent system A: H_2O; solvent system B: MeOH), to give compound **6** (16 mg, 67%) after freeze-drying. TLC R_f = 0.08 ($CHCl_3$/MeOH/AcOH/H_2O 60:30:5:3); ^1H NMR (400 MHz, D_2O/CD_3OD 1:4) δ 8.30 (1 H, s, H triazole), 8.28 (1 H, s, H triazole), 5.63 (1 H, d, *J* = 9.2 Hz, H-1'), 5.61 (1 H, d, *J* = 9.2 Hz, H-1''), 4.93 (1 H, d, *J* = 12.4 Hz, C*H*H), 4.85 (1 H, d, *J* = 12.4 Hz, C*H*H), 4.85 (1 H, d, *J* = 12.4 Hz, CH*H*), 4.74 (1 H, d, *J* = 12.4 Hz, CH*H*), 4.28 (1 H, t, *J* = 9.3 Hz, H-2'), 4.25 (1 H, br d, *J* = 3.4 Hz, H-4'), 4.22 (1 H, d, *J* = 7.6 Hz, H-1), 4.17 (1 H, t, *J* = 9.5 Hz, H-2''), 4.09 (1 H, br d, *J* = 3.1 Hz, H-4), 4.02 (1 H, br d, *J* = 3.1 Hz, H-4''), 3.92-3.86 (2 H, m, H-5 and H-5'), 3.80-3.69 (8 H, m, H-3', H-3'', 2 H-6, 2 H-6' and 2 H-6''), 3.60-3.54 (2 H, m, H-2 and H-5''), 3.53 (3 H, s, CH_3), 3.46 (1 H, dd, *J* = 3.2 and 9.7 Hz, H-3); ^{13}C NMR (100 MHz, D_2O/CD_3OD 1:4) δ 144.6 and 144.5 (2 C alkene), 123.1 (2 C alkene), 103.9 (C1), 88.3 and 88.2 (C-1' and C-1''), 80.9 and 80.8 (C-3 and C-3'), 78.2 and 78.0 (C-5 and C-5'), 74.8 (C-5''), 73.3 (C-3'), 69.7 (C-2 and C-2''), 68.8 (C-2'), 68.6 (C-4'), 65.3 and 65.1 (C-4 and C-4''), 61.9 and 61.6 (2 CH_2), 60.7 (C-6, C-6' and C-6''), 56.3 (CH_3); HR-ESI-MS *m/z* calculated for $C_{25}H_{40}N_6O_{16}$ $(M+Na)^+$ 703.2398, found 703.2433.

Methyl 3-*O*-(1-{3-*O*-[1-(3-propargyl β-D-galactopyranosyl)-1,2,3-triazol-4-yl]-methyl-β-D-galactopyranosyl}-1,2,3-triazol-4-yl)-methyl-β-D-galactopyranoside 7

To a solution of compound **1**(12 mg, 36 µmol) in H_2O/tBuOH (1:1) (200 µL), successive addition compound **6** (16 mg, 37 µmol), *o*-phenylenediamine (14 µL of a 375 mM aqueous solution), sodium ascorbate (14 µL of a 125 mM aqueous solution) and copper sulfate (14 µL

of a 125 mM aqueous solution), was done under argon. The reaction mixture was then stirred under darkness at RT overnight, then K_2CO_3 (10 mg, 73 µmol) and MeOH (200 µL) were added and the reaction mixture further stirred at RT for 1h30. The reaction mixture was concentrated under reduced pressure and the crude residue further purified by RP-HPLC (separation was performed on a Uptisphere Strategy 100 Å C18HQ (Interchim, France) (5 µm, 21.2 × 250 mm) column at a flow rate of 6 mL min^{-1} with ELSD and UV (225 nm) detection. Gradient: 0% B for 5 min, 0–50% B over 35 min; Solvent system A: H_2O; solvent system B: MeOH), to give compound **7** (16.2 mg, 46%) after freeze-drying. TLC R_f = 0.27 (CH_2Cl_2/MeOH 8:2);^{1}H NMR (400 MHz, CD_3OD) δ 8.26 (1 H, s, H triazole), 8.25 (1 H, s, H triazole), 5.65 (1 H, d, *J* = 9.0 Hz, H-1'), 5.63 (1 H, d, *J* = 9.2 Hz, H-1''), 4.94 (1 H, d, *J* = 12.4 Hz, C*H*H), 4.87 (1 H, d, *J* = 12.5 Hz, C*H*H), 4.86 (1 H, d, *J* = 12.4 Hz, CH*H*), 4.79 (1 H, d, *J* = 12.5 Hz, CH*H*), 4.47 (1 H, d, *J* = 15.7 Hz, C*H*H), 4.42 (1 H, d, *J* = 15.7 Hz, CH*H*), 4.30 and (2 H, 2 t, *J* = 9.3 Hz and *J* = 9.4 Hz, H-2' and H-2''), 4.25-4.22 (2 H, m, H-4' and H-4''), 4.18 (1 H, d, *J* = 7.7 Hz, H-1), 4.09 (1 H, br d, *J* = 3.0 Hz, H-4), 3.89-3.83 (2 H, m, H-5 and H-5'), 3.82-3.73 (7 H, m, H-3'', 2 H-6, 2 H-6' and 2 H-6''), 3.68 (1 H, dd, J = 3.1 and 9.6 Hz, H-3'), 3.64 (1 H, dd, *J* = 7.7 and 9.5 Hz, H-2), 3.54 (3 H, s, CH_3), 3.53-3.50 (1 H, m, H-5''), 3.42 (1 H, dd, *J* = 3.1 and 9.5 Hz, H-3); ^{13}C NMR (100 MHz, CD_3OD) δ 145.1 and 145.0 (2 C alkene), 122.3 (2 C alkene), 104.5 (C1), 88.8 (C-1' and C-1''), 81.7, 81.5 and 80.7 (C-3, C-3' and C-3''), 78.9 (C alkyne), 78.4 and 78.3 (C-5 and C-5'), 75.0 (C-5''), 74.6 (C alkyne), 70.2, 69.2 and 69.1 (C-2, C-2' and C-2''), 66.0, 65.7 and 65.5 (C-4, C-4' and C-4''), 62.4 and 62.1 (2 CH_2), 61.1, 61.0 and 60.9 (C-6, C-6' and C-6''), 56.8 (CH_2), 55.8 (CH_3); HR-ESI-MS *m/z* calculated for $C_{28}H_{42}N_6O_{16}$ $(M+Na)^+$ 741.2550, found 741.2523.

Methyl 3-*O*-(1-{3-*O*-[1-(1-(β-D-galactopyranosyl)-1,2,3-triazol-4-yl]-methyl-β-D-galactopyranosyl)-1,2,3-triazol-4-yl]-methyl-β-D-galactopyranosyl}-1,2,3-triazol-4-yl)-methyl-β-D-galactopyranoside 8

To a solution of compound **1** (0.86 mg, 4.19 µmol) in H_2O/tBuOH (1:1) (16 µL), successive addition of **7** (3 mg, 4.17 µmol), *o*-phenylenediamine (1.1 µL of a 375 mM aqueous solution), sodium ascorbate (1.1 µL of a 125 mM aqueous solution) and copper sulfate (1.1 µL of a 125 mM aqueous solution), was undertaken under argon. The reaction mixture was then stirred under darkness at RT overnight. The reaction mixture was concentrated under reduced pressure and further purified by RP-HPLC (separation was performed on a Uptisphere Strategy 100 Å C18HQ (Interchim, France) (5 µm, 21.2 × 250 mm) column at a flow rate of 6 mL min^{-1} with

ELSD and UV (225 nm) detection. Gradient: 0% B for 5 min, 0–50% B over 35 min; Solvent system A: H_2O; solvent system B: MeOH), to give compound **8** (2.13 mg, 55%) after freeze-drying. TLC R_f = 0.35 (BuOH/EtOH/H_2O 5:5:3); ^{1}H NMR (400 MHz, D_2O) δ 8.30 (2 H, s, 2 H triazole), 8.27 (1 H, s, H triazole), 5.70, 5.69 and 5.68 (3 H, 3 d, *J* = 9.0, 9.2 and 9.1 Hz, H-1', H-1'' and H-1'''), 4.92, 4.91 and 4.84 (3 H, 3 d, *J* = 12.6, 12.5 and 12.3 Hz, 3 C*H*H), 4.81, 4.81 and 4.73 (3 H, 3 d, *J* = 12.6, 12.5 and 12.3 Hz, 3 CH*H*), 4.31-4.26 (4 H, m, H-1, H-2', H-2''and H-4'), 4.24 (1 H, br d, *J* = 3.7 Hz, H-4''), 4.20 (1 H, t, *J* = 9.7 Hz, H-2'''), 4.07 (1 H, br d, *J* = 2.0 Hz, H-4), 4.05 (1 H, br d, *J* = 3.1 Hz, H-4'''), 3.99-3.94 (3 H, m, H-5, H-5' and H-5''), 3.85-3.67 (13 H, m, H-3', H-3'', H-3''', 2 H-6, 2 H-6', 2 H-6'' and 2 H-6'''), 3.63 (1 H, dd, *J* = 4.2 and 7.9 Hz, H-2), 3.54-3.51 (2 H, m, H-3 and H-5'''); HR-ESI-MS *m/z* calculated for $C_{34}H_{53}N_9O_{21}(M+Na)^+$ 946.3254, found 946.3269.

2.3 | Expression and purification of full length galectin- 3, and galectin-3 CRD, proteins

Production of full-length galectin-3 was carried out in *E. coli* BL21(DE3) strain transformed by construction in pTRC expression vector overnight cultured in LB-ampicillin medium supplemented with 1 mM Isopropyl β-D-1-thiogalactopyranoside (IPTG), at 20°C. After protein extraction (Avestin emulsiflex C5; 15000psi) in a 20 mM phosphate–150 mM NaCl buffer pH7.35, (1 mM of PMSF, 2 mM EDTA, 4 mM DTT) purification is realized by column chromatography with a lactose agarose matrix (Sigma-Aldrich; L7634) at 4°C. Elution fractions (100mM of lactose) were further purified by size-exclusion chromatography on a Superdex 75 column (GE Healthcare) to eliminate lactose. Galectin-3 CRD (amino acid residues 108-250) was generated and purified in its untagged form as described previously.(Collins et al., 2007) Briefly, bacterial culture were induced at OD 0.6 with 1mM IPTG and grown for 3-4 hours at 37°C. Bacterial cells were lysed, and galectin-3 CRD was purified through affinity chromatography on a lactosyl-sepharose column. Elution was performed at 100 mM lactose, and extensive dialysis was performed in 1×PBS to remove lactose. Finally, protein was concentrated to 11 mg/ml and flash cryo-cooled at liquid nitrogen prior to storage at minus 80°C.

2.4 Crystallization

Galectin-3 CRD protein crystals were obtained using the hanging-drop vapour-diffusion method after the mixing of a 1:1 ratio of galectin-3 CRD (11mg/ml) and the reservoir solution (31% PEG 3100, 100 mM tris-HCl pH 7.5, 100 mM $MgCl_2$, 8 mM 2-Mercaptoethanol).

Crystals grew within 2 weeks. Galectin-3 CRD complexes with either **4** or **6** were obtained by soaking the crystal in reservoir solution that contained 100 mM of either compound. X-ray diffraction data sets were collected at 100 K at beamline MX1 of the Australian Synchrotron. Data were integrated using iMOSFLM and scaled and merged using SCALA, as implemented in the CCP4 suite of crystallographic software.(Winn, 2011) The atomic structures of the galectin-3 CRD **4** and **6** complexes were solved by molecular replacement using a search model of the galectin-3 CRD (PDB ID: 2NMO(Collins, 2007)) and REFMAC5 was used for atomic model refinement.(Murshudov, 1997) Visualization of electron densities and model building was performed using COOT.(Emsley et al., 2010) Ligand geometry was obtained using the PRODRG2 server.(Schüttelkopf, 2004)

2.5 | Fluorescence polarization analysis

Fluorescence polarization experiments were carried out using full length galectin-3 as described in the supplementary information and in the literature.(Dion, 2017)

3 | RESULTS

3.1 | Synthesis of inhibitors

An iterative synthesis has been designed to prepare a set of oligo-galactosides using two terminating, and one elongating, building blocks **1-3** (Scheme 1). The latter was obtained upon reacting 1-azido-1-deoxy-β-D-galactopyranose **1** with 3-bromo-1(trimethylsilyl)-1-propyne from O3-O4 stannylidene intermediate in 68% yield. Cu(I)-catalyzed azide–alkyne cycloaddition of building block **1** with **2** in the presence of o-phenylenediamine(Baron et al., 2008) gave rise to known disaccharide **4**(Xu et al., 2016) in 76% yield. Application of these conditions to the cycloaddition of galactoside **3** with **1** was accompanied with the loss of the trimethylsilyl protecting group to give rise to disaccharide **5** in 47% yield. Compound **5** was next reacted analogously with either **1** or **3** to provide trisacccharides **6** or **7** in 55 and 46% yield, respectively. Finally, tetrasaccharide **8** was obtained in 67% yield from **7** and terminating building block **1**.

3.2 | Affinity studies

The binding affinities of galectin-3 for **4**–**8** and the reference compounds methyl β-D-galactoside **9**, $(LacNAc)_2$ **10** and $(LacNAc)_3$ **11** (Figure 1) were evaluated by a fluorescent polarization assay (Table 1). Very weak affinities were determined for methyl β-D-galactoside

6 as well as for **4,** which is consistent with reported data in the literature.(Rajput et al., 2014) The K_d of galectin-3 for di-galactosides decreased about 17 times to 1.2 mM. The tendency is further confirmed for tri-galactosides **6** and **7** as well as tetra-galactoside **8** to reach 500 μM. The K_d values for $(LacNAc)_2$ and $(LacNAc)_3$ were much stronger and determined to be 5 μM and 3 μM respectively $(LacNAc)_2$ and $(LacNAc)_3$. These values are in good agreement with those reported for derivatized-$LacNAc)_2$ and $(LacNAc)_3$ analogs reported in the literature (1.3 and 0.35 μM, respectively), and determined by frontal affinity chromatography.(Hirabayashi et al., 2002)

3.3 | Crystal structure of galectin-3 CRD in complex with compounds 4 and 6

The crystal structures of galectin-3 CRD with compound **4** and with **6**, reveal that in both cases galactose at the non-reducing (upstream) end and adjacent triazole ring could bind within the carbohydrate recognition site via a stacking interaction with W181 and combined with a series of hydrogen bonding interactions with the CRD subsite C residues. The binding mode of the ring of this galactose exhibits characteristic interactions exhibited by galectins with galactose when integrated as a component of endogenous ligands for example lactose (Figure 2A). The interactions between galectin-3 CRD and galactose ring are consistent and also observed in structures of galectin-3 CRD with bound galactose-based derivatives.(Collins, 2007),(Kishor, 2018),(Atmanene, 2017)

The triazole ring linked to the upstream end in both compound **4** and **6** participated in the hydrogen bonding with the side chain of R162 and a water molecule *W1*. The *W1* helps the triazole ring to further interact with the CRD site via hydrogen bonds with R186 and E184.

The electron density map for the upstream galactose and triazole ring portion of the molecule is well-defined and reveals that it is this end of oligogalactosides that makes the key interactions with galectin-3 through the formation of a stable conformation. In contrast, the downstream region of the molecule is not significantly visible in the omit electron density map (at 1.0 σ) due to flexibility resulting in multiple conformations. However, at lower electron density contour levels (~0.7 σ) there is indication of the direction that the downstream galactose ring of compound **4,** and the central galactose ring of compound **6,** could position, which is such that there could be interaction with the side chain of E165. Besides this, the electron density for the downstream galactose ring of compound **6** could not be traced. The upstream end of compounds **4** and **6** have a galactose covalently linked to a triazole ring and this forms a rigid conformation that could be accommodated in the carbohydrate binding site of galectin-3. However, the 1-4 glycosidic bond to the N-acetyllactosamine (LacNAc) (compounds **10** and **11**) exhibits more flexibility than a triazole ring (such as within compounds **4** and **6**), and the

GlcNAc moiety could bend toward subsite D and interact with galectin-3 more strongly (Figure 2D), which was reflected through the FP assay where $(LacNAc)_2$ and $(LacNAc)_3$ affinity is estimated to be 5 and 3 μM for galectin-3. Conversely, the electron density map of the downstream end of the galactose ring in compound **4** and triazole-linked galactose in compound **6** could not be traced (Figure 2A and 2B). The flexibility of the downstream end of both compounds could be a reason for lack of electron density for this end (Figure 2C). However, the downstream end in compound **6** is longer and anticipated more flexible than compound **4** and thus has more ability to provide additional interactions by fitting in the groove between residues R168 and S188 (Figure 2D). The shorter downstream end of compound **4** has restricted access to reach that groove (Figure 2D). This could explain the binding affinity results which reveal that the tri-galactosides (compound **6**) binds significantly tighter than mono galactosides (compound **2**) and di- galactosides (compound **4**) for galectin-3 (Table1).

4 | DISCUSSION

Galectin-3 binds with exquisite specificity to poly-*N*-acetyllactosamines which are expressed as natural motifs on glycans at mammalian cell surfaces. This recognition facilitates cancer progression and immune cell evasion.(Bresalier, 1996),(Srinivasan, 2009),(Dange, 2014),(Tsuboi, 2011) We have herein developed bioinspired synthetic inhibitors to selectively target galectin-3 whereby GlcNAc units of poly-*N*-acetyllactosamine are replaced by 1,2,3-triazoles while keeping the galactoside residues. Preparation of these linear triazole-linked *pseudo* oligogalactosides relies on click-chemistry reactions using a limited number of three different building blocks and thus is straightforward and cost effective. The 1,2,3-triazole ring is well established as a bioisostere notably as an amide, carboxylic acid and ester surrogates (Bonandi, 2017) Of note is that a sugar triazolyl nucleoside has been synthesized as a nucleoside triphosphate mimic and shown to be an ATP-competitive inhibitor.(Rowan, 2009) On the other hand linear or cyclic 1,2,3-triazole *pseudo* oligosaccharide have been reported but with the aim of obtaining new materials or to be used as scaffolds.(Schmidt, 2016),(Temelkoff, 2006),(Pathigoolla, 2013),(Campo, 2015) In one case, triazoles were used as mannose surrogates in the development of high mannose mimics but they most likely serve as spacers.(François-Heude, 2015) This is the case when click-chemistry has been applied for design of galectin inhibitors.(Marchiori, 2015),(André, 2014),(Giguère, 2008) Five *pseudo* oligogalactosides have been synthesized and the galectin-3 CRD's affinity for these compounds has been assessed. They appeared to be weak inhibitor of the galectin-3. However, the actual affinities show stronger binding for these derivatives than for methyl β-D-galactopyranoside.

Affinities increased from the mono up to the di- and further to the tri-galactoside Affinities of digalactosides **4** or **5** for the galectin-3 are comparable to that of an analogous head-to-head digalactoside inhibitor, previously reported in the literature whereby the triazole ring was introduced as a spacer.(Giguère, 2008) Moreover, the observed affinities are higher than those determined for galactoside clusters based on RAFT or lysine tree scaffolds.(André, 2011),(André, 2000) However, these observations are unlikely to be ascribed to a multivalency effect since the topology of the oligogalactosides does not allow the bridging of the CRD of two distinct galectin-3 molecules. $(LacNAc)_2$ and $(LacNAc)_3$ are two natural galectin-3 linear oligosaccharide ligands composed of two and three galactoses respectively, and which have been included as positive controls in our assay. They proved to be 100 times more potent towards the galectin-3 than the herein tested *pseudo* oligogalactosides. While galactose binds weakly to the galectin-3 CRD, notably via an O4 and O6 hydrogen bonding network, and upon establishing hydrogen-π interactions with residue W181 of the CRD, GlcNAc alone does not bind at all with the galectin-3 CRD. However, when the latter is linked to a galactose residue *e.g.* as in lactose/lactosamine type I or type II core (Galβ1-3GlcNAc or Galβ1-4GlcNAc), both sugars cooperate to create an extensive hydrogen bonding and salt bridge network, resulting in a micromolar range affinity.(Hsieh, 2015),(Atmanene, 2017) Extension of this core with further LacNAc unit leads to additional interaction and subsequently improved binding. The 1,2,3-triazole ring is obviously too rigid and not functionalized to be a true mimic of a GlcNAc residue. To explain the observed affinities which are intermediate between that of galactose and those of $(LacNAc)_2$ and $(LacNAc)_3$, one could evoke a "bind and slide"(Dam, 2008) binding or galactose rebinding mechanisms due to higher local concentration. Additional stabilizing interactions provided by the oligogalactosides compared to monogalactosides would be an even simpler explanation. For example, it is well established that 1,2,3-triazole ring substituents at the C3 position of the galactose can occupy subsite B or the galectin-3 CRD and contribute to the stabilization of galactose/lactose derivatives within the CRD.(Salameh, 2010) Finally, these novel inhibitors could interact through a different mechanisms. We thus carried out crystallographic studies of galectin-3 CRD in complex with di- and tri-galactosides **4** and **6** to gain insights into their mode of binding. The crystal structure of the galectin-3 CRD complex with compound **4** and **6** reveals that galactose linked with a triazole ring at the non-reducing end could be accommodated in the CRD binding site (subsite C) while the downstream end of both compounds are directed toward subsite E, with the longer compound **6** being able to occupy that subsite. The triazole ring at the upstream end could be providing a rigidity to the galactose moiety to bind with CRD of galectin-3. The downstream galactose ring of compound

6 could reach the groove present between R168 and S188 providing additional interactions. The revelation of the features of binding of triazole-linked oligogalactoside will assist in designing better inhibitors with high affinity for galectins.

5 | CONCLUSION

Galectins are key to maintain homeostasis. They have essential roles in various biological processes in normal but also in pathological conditions, a feature which makes them potential therapeutic targets. Galectins exert their activities upon binding to carbohydrate motifs through a small set of six extremely conserved residues in their CRDs. A major challenge thus remains in the design of inhibitors that are specific for each individual galectin, which is an important aim since they can play distinct roles, sometimes antagonist. In search of galectin binders, we have reported herein that oligo triazolo-galactosides are new scaffolds able to accommodate galectin-3 binding site. The rigidity of these unprecedented structures does not allow a perfect fitting with the galectin-3 CRD but could be advantageously exploited to introduce substituents at defined positions and gain further interactions, providing higher affinity.

DATA AVAILABILTY STATEMENT

Absence of shared data

CONFLICT OF INTEREST

The authors of this manuscript declare no conflict of interests.

ORCID

ORCID Cyrille Grandjean http://orcid.org/0000-0002-9775-6917
ORCID Helen Blanchard http://orcid.org/0000-0003-3372-5027
ORCID Chandan Kishor https://orcid.org/0000-0002-6328-1116

4 | REFERENCES

André, S., Frisch, B., Kaltner, H., Desouza, D. L., Schuber, F., & Gabius, H. J. (2000). Lectin-mediated drug targeting : Selection of valency, sugar type (Gal/Lac), and spacer length for cluster glycosides as parameters to distinguish ligand binding to C-type asialoglycoprotein receptors and galectins. *Pharm. Res.*, *17*(8), 985-990.

André, Sabine, Renaudet, O., Bossu, I., Dumy, P., & Gabius, H.-J. (2011). Cyclic neoglycodecapeptides : How to increase their inhibitory activity and selectivity on lectin/toxin binding to a glycoprotein and cells. *J. Peptide Sci., 17*(6), 427‑437. https://doi.org/10.1002/psc.1338

André, Sabine, Wang, G.-N., Gabius, H.-J., & Murphy, P. V. (2014). Combining glycocluster synthesis with protein engineering : An approach to probe into the significance of linker length in a tandem-repeat-type lectin (galectin-4). *Carbohydr. Res.*, *389*, 25‑38. https://doi.org/10.1016/j.carres.2013.12.024

Atmanene, C., Ronin, C., Téletchéa, S., Gautier, F.-M., Djedaïni-Pilard, F., Ciesielski, F., Vivat, V., & Grandjean, C. (2017). Biophysical and structural characterization of mono/di-arylated lactosamine derivatives interaction with human galectin-3. *Biochem. Biophys. Res. Commun.*, *489*(3), 281‑286. https://doi.org/10.1016/j.bbrc.2017.05.150

Baron, A., Blériot, Y., Sollogoub, M., & Vauzeilles, B. (2008). Phenylenediamine catalysis of « click glycosylations » in water : Practical and direct access to unprotected neoglycoconjugates. *Org. Biomol. Chem.*, *6*(11), 1898‑1901. https://doi.org/10.1039/b805528a

Barondes, S. H., Castronovo, V., Cooper, D. N., Cummings, R. D., Drickamer, K., Feizi, T., Gitt, M. A., Hirabayashi, J., Hughes, C., & Kasai, K. (1994). Galectins : A family of animal beta-galactoside-binding lectins. *Cell*, *76*(4), 597‑598.

Bian, C.-F., Zhang, Y., Sun, H., Li, D.-F., & Wang, D.-C. (2011). Structural basis for distinct binding properties of the human galectins to Thomsen-Friedenreich antigen. *PloS One*, *6*(9), e25007. https://doi.org/10.1371/journal.pone.0025007

Bonandi, E., Christodoulou, M. S., Fumagalli, G., Perdicchia, D., Rastelli, G., & Passarella, D. (2017). The 1,2,3-triazole ring as a bioisostere in medicinal chemistry. *Drug Discov. Today*, *22*(10), 1572‑1581. https://doi.org/10.1016/j.drudis.2017.05.014

Bresalier, R. S., Byrd, J. C., Wang, L., & Raz, A. (1996). Colon cancer mucin : A new ligand for the beta-galactoside-binding protein galectin-3. *Cancer Res.*, *56*(19), 4354-4357.

Campo, V. L., Ivanova, I. M., Carvalho, I., Lopes, C. D., Carneiro, Z. A., Saalbach, G., Schenkman, S., da Silva, J. S., Nepogodiev, S. A., & Field, R. A. (2015). Click chemistry oligomerisation of azido-alkyne-functionalised galactose accesses triazole-linked linear oligomers and macrocycles that inhibit *Trypanosoma cruzi* macrophage invasion. *Tetrahedron*, *71*(39), 7344-7353. https://doi.org/10.1016/j.tet.2015.04.085

Collins, P. M., Bum-Erdene, K., Yu, X., & Blanchard, H. (2014). Galectin-3 interactions with glycosphingolipids. *J. Mol. Biol.*, *426*(7), 1439-1451. https://doi.org/10.1016/j.jmb.2013.12.004

Collins, P. M., Hidari, K. I. P. J., & Blanchard, H. (2007). Slow diffusion of lactose out of galectin-3 crystals monitored by X-ray crystallography : Possible implications for ligand-exchange protocols. *Acta Crystallogr. Sect. D, Biol. Crystallogr.*, *63*(Pt 3), 415-419. https://doi.org/10.1107/S090744490605270X

Dam, T. K., & Brewer, C. F. (2008). Effects of clustered epitopes in multivalent ligand-receptor interactions. *Biochemistry*, *47*(33), 8470-8476. https://doi.org/10.1021/bi801208b

Dange, M. C., Srinivasan, N., More, S. K., Bane, S. M., Upadhya, A., Ingle, A. D., Gude, R. P., Mukhopadhyaya, R., & Kalraiya, R. D. (2014). Galectin-3 expressed on different lung compartments promotes organ specific metastasis by facilitating arrest, extravasation and organ colonization via high affinity ligands on melanoma cells. *Clin. Exp. Metastasis*, *31*(6), 661-673. https://doi.org/10.1007/s10585-014-9657-2

Delaine, T., Collins, P., MacKinnon, A., Sharma, G., Stegmayr, J., Rajput, V. K., Mandal, S., Cumpstey, I., Larumbe, A., Salameh, B. A., Kahl-Knutsson, B., van Hattum, H., van Scherpenzeel, M., Pieters, R. J., Sethi, T., Schambye, H., Oredsson, S., Leffler, H.,

Blanchard, H., & Nilsson, U. J. (2016). Galectin-3-Binding Glycomimetics that Strongly Reduce Bleomycin-Induced Lung Fibrosis and Modulate Intracellular Glycan Recognition. *Chembiochem*, *17*(18), 1759‑1770. https://doi.org/10.1002/cbic.201600285

Dion, J., Advedissian, T., Storozhylova, N., Dahbi, S., Lambert, A., Deshayes, F., Viguier, M., Tellier, C., Poirier, F., Téletchéa, S., Dussouy, C., Tateno, H., Hirabayashi, J., & Grandjean, C. (2017). Development of a Sensitive Microarray Platform for the Ranking of Galectin Inhibitors : Identification of a Selective Galectin-3 Inhibitor. *Chembiochem*, *18*(24), 2428‑2440. https://doi.org/10.1002/cbic.201700544

Dubé-Delarosbil, C., & St-Pierre, Y. (2018). The emerging role of galectins in high-fatality cancers. *Cell. Mol. Life Sciences: CMLS*, *75*(7), 1215‑1226. https://doi.org/10.1007/s00018-017-2708-5

Emsley, P., Lohkamp, B., Scott, W. G., & Cowtan, K. (2010). Features and development of Coot. *Acta Crystallogr. Sect. D, Biol. Crystallogr.*, *66*(Pt 4), 486‑501. https://doi.org/10.1107/S0907444910007493

Fischöder, T., Laaf, D., Dey, C., & Elling, L. (2017). Enzymatic Synthesis of N-Acetyllactosamine (LacNAc) Type 1 Oligomers and Characterization as Multivalent Galectin Ligands. *Molecules*, *22*(8). https://doi.org/10.3390/molecules22081320

Fort, S., Kim, H.-S., & Hindsgaul, O. (2006). Screening for galectin-3 inhibitors from synthetic lacto-N-biose libraries using microscale affinity chromatography coupled to mass spectrometry. *J. Org. Chem.*, *71*(19), 7146‑7154. https://doi.org/10.1021/jo060485v

François-Heude, M., Méndez-Ardoy, A., Cendret, V., Lafite, P., Daniellou, R., Ortiz Mellet, C., García Fernández, J. M., Moreau, V., & Djedaïni-Pilard, F. (2015). Synthesis of high-mannose oligosaccharide analogues through click chemistry : True functional

mimics of their natural counterparts against lectins? *Chemistry*, *21*(5), 1978-1991. https://doi.org/10.1002/chem.201405481

Giguère, D., Bonin, M.-A., Cloutier, P., Patnam, R., St-Pierre, C., Sato, S., & Roy, R. (2008). Synthesis of stable and selective inhibitors of human galectins-1 and -3. *Bioorg. Med. Chem.*, *16*(16), 7811-7823. https://doi.org/10.1016/j.bmc.2008.06.044

Hirabayashi, J., Hashidate, T., Arata, Y., Nishi, N., Nakamura, T., Hirashima, M., Urashima, T., Oka, T., Futai, M., Muller, W. E. G., Yagi, F., & Kasai, K. (2002). Oligosaccharide specificity of galectins : A search by frontal affinity chromatography. *Biochim. Biophys. Acta*, *1572*(2-3), 232-254.

Hsieh, T.-J., Lin, H.-Y., Tu, Z., Huang, B.-S., Wu, S.-C., & Lin, C.-H. (2015). Structural Basis Underlying the Binding Preference of Human Galectins-1, -3 and -7 for Galβ1-3/4GlcNAc. *PloS One*, *10*(5), e0125946. https://doi.org/10.1371/journal.pone.0125946

Johannes, L., Jacob, R., & Leffler, H. (2018). Galectins at a glance. *J. Cell Sci.*, *131*(9). https://doi.org/10.1242/jcs.208884

Kishor, C., Ross, R. L., & Blanchard, H. (2018). Lactulose as a novel template for anticancer drug development targeting galectins. *Chem. Biol. Drug Des.*, *92*(4), 1801-1808. https://doi.org/10.1111/cbdd.13348

Knibbs, R. N., Agrwal, N., Wang, J. L., & Goldstein, I. J. (1993). Carbohydrate-binding protein 35. II. Analysis of the interaction of the recombinant polypeptide with saccharides. *J. Biol. Chem.*, *268*(20), 14940-14947.

Leffler, H., & Barondes, S. H. (1986). Specificity of binding of three soluble rat lung lectins to substituted and unsubstituted mammalian beta-galactosides. *J. Biol. Chem.*, *261*(22), 10119-10126.

Marchiori, M. F., Souto, D. E. P., Bortot, L. O., Pereira, J. F., Kubota, L. T., Cummings, R. D., Dias-Baruffi, M., Carvalho, I., & Campo, V. L. (2015). Synthetic 1,2,3-triazole-

linked glycoconjugates bind with high affinity to human galectin-3. *Bioorg. Med. Chem.*, *23*(13), 3414-3425. https://doi.org/10.1016/j.bmc.2015.04.044

Murshudov, G. N., Vagin, A. A., & Dodson, E. J. (1997). Refinement of macromolecular structures by the maximum-likelihood method. *Acta Crystallogr. Sect. D, Biol. Crystallogr.*, *53*(Pt 3), 240-255. https://doi.org/10.1107/S0907444996012255

Nagae, M., Nishi, N., Murata, T., Usui, T., Nakamura, T., Wakatsuki, S., & Kato, R. (2009). Structural analysis of the recognition mechanism of poly-N-acetyllactosamine by the human galectin-9 N-terminal carbohydrate recognition domain. *Glycobiology*, *19*(2), 112-117. https://doi.org/10.1093/glycob/cwn121

Oberg, C. T., Leffler, H., & Nilsson, U. J. (2011). Inhibition of galectins with small molecules. *Chimia*, *65*(1-2), 18-23.

Pathigoolla, A., & Sureshan, K. M. (2013). A crystal-to-crystal synthesis of triazolyl-linked polysaccharide. *Angew. Chem. Int. Ed.*, *52*(33), 8671-8675. https://doi.org/10.1002/anie.201303372

Rajput, V. K., Leffler, H., Nilsson, U. J., & Mukhopadhyay, B. (2014). Synthesis and evaluation of iminocoumaryl and coumaryl derivatized glycosides as galectin antagonists. *Bioorg. Med. Chem. Lett.*, *24*(15), 3516-3520. https://doi.org/10.1016/j.bmcl.2014.05.063

Rowan, A. S., Nicely, N. I., Cochrane, N., Wlassoff, W. A., Claiborne, A., & Hamilton, C. J. (2009). Nucleoside triphosphate mimicry : A sugar triazolyl nucleoside as an ATP-competitive inhibitor of B. anthracis pantothenate kinase. *Org. Biomol.Chem.*, *7*(19), 4029-4036. https://doi.org/10.1039/b909729e

Salameh, B. A., Cumpstey, I., Sundin, A., Leffler, H., & Nilsson, U. J. (2010). 1H-1,2,3-triazol-1-yl thiodigalactoside derivatives as high affinity galectin-3 inhibitors. *Bioorg. Med. Chem.*, *18*(14), 5367-5378. https://doi.org/10.1016/j.bmc.2010.05.040

Sauerzapfe, B., Krenek, K., Schmiedel, J., Wakarchuk, W. W., Pelantová, H., Kren, V., & Elling, L. (2009). Chemo-enzymatic synthesis of poly-N-acetyllactosamine (poly-LacNAc) structures and their characterization for CGL2-galectin-mediated binding of ECM glycoproteins to biomaterial surfaces. *Glycoconj. J.*, *26*(2), 141-159. https://doi.org/10.1007/s10719-008-9172-2

Schmidt, M. S., Götz, K. H., Koch, W., Grimm, T., & Ringwald, M. (2016). Studies toward the synthesis of linear triazole linked pseudo oligosaccharides and the use of ferrocene as analytical probe. *Carbohydr. Res.*, *425*, 28-34. https://doi.org/10.1016/j.carres.2016.03.005

Schüttelkopf, A. W., & van Aalten, D. M. F. (2004). PRODRG : A tool for high-throughput crystallography of protein-ligand complexes. *Acta Crystallograph.. Sect. D, Biol. Crystallogr.*, *60*(Pt 8), 1355-1363. https://doi.org/10.1107/S0907444904011679

Sciacchitano, S., Lavra, L., Morgante, A., Ulivieri, A., Magi, F., De Francesco, G. P., Bellotti, C., Salehi, L. B., & Ricci, A. (2018). Galectin-3 : One Molecule for an Alphabet of Diseases, from A to Z. *Int. J. Mol. Sciences*, *19*(2). https://doi.org/10.3390/ijms19020379

Srinivasan, N., Bane, S. M., Ahire, S. D., Ingle, A. D., & Kalraiya, R. D. (2009). Poly N-acetyllactosamine substitutions on N- and not O-oligosaccharides or Thomsen-Friedenreich antigen facilitate lung specific metastasis of melanoma cells via galectin-3. *Glycoconj. J.*, *26*(4), 445-456. https://doi.org/10.1007/s10719-008-9194-9

Temelkoff, D. P., Zeller, M., & Norris, P. (2006). N-glycoside neoglycotrimers from 2,3,4,6-tetra-O-acetyl-beta-D-glucopyranosyl azide. *Carbohydr. Res.*, *341*(9), 1081-1090. https://doi.org/10.1016/j.carres.2006.04.011

Toscano, M. A., Martínez Allo, V. C., Cutine, A. M., Rabinovich, G. A., & Mariño, K. V. (2018). Untangling Galectin-Driven Regulatory Circuits in Autoimmune

Inflammation. *Trends Mol. Medicine*, *24*(4), 348-363. https://doi.org/10.1016/j.molmed.2018.02.008

Tsuboi, S., Sutoh, M., Hatakeyama, S., Hiraoka, N., Habuchi, T., Horikawa, Y., Hashimoto, Y., Yoneyama, T., Mori, K., Koie, T., Nakamura, T., Saitoh, H., Yamaya, K., Funyu, T., Fukuda, M., & Ohyama, C. (2011). A novel strategy for evasion of NK cell immunity by tumours expressing core2 O-glycans. *EMBO J.*, *30*(15), 3173-3185. https://doi.org/10.1038/emboj.2011.215

van Hattum, H., Branderhorst, H. M., Moret, E. E., Nilsson, U. J., Leffler, H., & Pieters, R. J. (2013). Tuning the preference of thiodigalactoside- and lactosamine-based ligands to galectin-3 over galectin-1. *J. Med. Chem.*, *56*(3), 1350-1354. https://doi.org/10.1021/jm301677r

Winn, M. D., Ballard, C. C., Cowtan, K. D., Dodson, E. J., Emsley, P., Evans, P. R., Keegan, R. M., Krissinel, E. B., Leslie, A. G. W., McCoy, A., McNicholas, S. J., Murshudov, G. N., Pannu, N. S., Potterton, E. A., Powell, H. R., Read, R. J., Vagin, A., & Wilson, K. S. (2011). Overview of the CCP4 suite and current developments. *Acta Crystallogr. Sect. D, Biol. Crystallogr.*, *67*(Pt 4), 235-242. https://doi.org/10.1107/S0907444910045749

Xu, H., Ren, B., Zhao, W., Xin, X., Lu, Y., Pei, Y., Dong, H., & Pei, Z. (2016). Regioselective mono and multiple alkylation of diols and polyols catalyzed by organotin and its applications on the synthesis of value-added carbohydrate intermediates. *Tetrahedron*, *72*(24), 3490-3499. https://doi.org/10.1016/j.tet.2016.04.076

Zetterberg, F. R., Peterson, K., Johnsson, R. E., Brimert, T., Håkansson, M., Logan, D. T., Leffler, H., & Nilsson, U. J. (2018). Monosaccharide Derivatives with Low-Nanomolar Lectin Affinity and High Selectivity Based on Combined Fluorine-Amide,

Phenyl-Arginine, Sulfur-π, and Halogen Bond Interactions. *ChemMedChem*, *13*(2), 133-137. https://doi.org/10.1002/cmdc.201700744

TABLE 1. K_d (mM)¶ values of galactoside derivatives and reference compounds for galectin-3 at 4°C†

Compound	**9** Me β-Gal	**2**	**4**	**5**§	**6**	**7**§	**10** (LacNAc)$_2$	**8**	**11** (LacNAc)$_3$
K_d	>4 000	4 000	972 ±144	1170 ±370	535 ±138	379±102	3.76 ±0.73	372 ±55	2.60 ±0.51
β factor / **2**‡	-	1	1.6	1.7	2	3.5	400	2	444

¶Average and standard deviation of repeated point measurements;†Determined by fluorescence polarization (see SI); ‡β factor is calculated as K_d for **2** / (K_d for a given inhibitor × number of galactose residues) to take into account of the numbers of galactose per derivative; §Purity of compounds **5** and **7** was 85% and 93%, respectively, as estimated by their respective ^{1}H NMR spectra.

TABLE 2. Crystallographic data and refinement statistics.

Parameter	**Galectin-3 CRD in complex with compound 4**	**Galectin-3 CRD in complex with compound 6**
Data collection		
Resolution range (Å)	31.3-1.99 (2.06-1.99)	42.41 - 1.99 (2.06 - 1.99)
Space group	$P2_12_12_1$	$P2_12_12_1$
Unit cell	*a*=35.74, *b*=57.82 *c*=62.59	*a*=35.95, *b*= 57.86 *c*=62.34
Total reflections	108810 (3288)	72928 (2202)
Unique reflections	9346 (906)	9367 (901)
Multiplicity	11.5	7.7
Completeness (%)	100 (99.9)	99.9 (99.5)
Mean I/sigma(I)	27.0 (8.1)	49.6 (17.6)
Wilson B-factor	11.65	11.97
R-merge (%)	6.7 (11.7)	2.9 (5.3)
Refinement Statistics		
R-work (%)	16.41 (18.1)	17.86 (19.6)
R-free (%)	20.53 (21.2)	21.75 (24.3)
RMS deviations		
RMS (bonds)	0.016	0.020
RMS (angles)	2.03	2.14
Ramachandran plot statistics (%)		
Favoured	96.6	97.2
Allowed	3.4	2.8
Outliers	0	0
PDB ID	6Q17	6Q0Q

$^{\#}R_{merge} = \sum_{hkl}\sum_{i}|I_i(hkl) - (I(hkl))| / \sum_{hkl}\sum_{i} I_i(hkl)$

FIGURE LEGENDS

Scheme 1. Synthesis of mono-, di-, tri- and tetragalactosides. Reagent and conditions: a) $CuSO_4$ (5 mol%), sodium ascorbate (10 mol%), o-phenylenediamine (15 mol%), H_2O-tBuOH (1:1), RT, overnight.

Figure 1. Reference compounds: Methyl β-D-galactopyranoside **9** and di- and tri-lactosamine **10** and **11**

Figure 2. A) Stereo diagram of the $2\left|F_o\right| - \left|F_c\right| \alpha_c$ map of compound **4** (at 1 σ) (yellow stick) (PDB ID 6Q17) bound within the galectin-3 CRD. Galectin-3 is depicted as a grey ribbon and interacting residues indicated as a grey sticks, hydrogen bonds indicated as a dashed black line. The water molecules interacting with compound **4** indicated as red spheres. B) Stereo diagram of the $2\left|F_o\right| - \left|F_c\right|$ of compound **6** (cyan stick) (PDB ID 6Q0Q) at 1 σ at CRD binding site of galectin-3. C) Alignment of the crystal structures of galectin-3 CRD in complex with **4** and **6** showing the upstream galactose and triazole rings could fit into the carbohydrate recognition site of the galectin-3 CRD whilst the downstream substituents adopt orientation toward subsite E. D) Comparison of compounds **4** and **6** with N-acetyllactosamine (LacNAc as a purple blue stick) (PDB ID:1KJL)[47] in CRD of galectin-3 to indicate that the 1-4 glycosidic of LacNac is more flexible and bend toward subsite D. The downstream galactose ring of compound **4** and the central galactose ring of compound **6** bend towards subsite E whilst the downstream galactose ring of compound **6** extends from subsite E and could approach the groove (red oval circle) between R168 and S188 for additional binding.

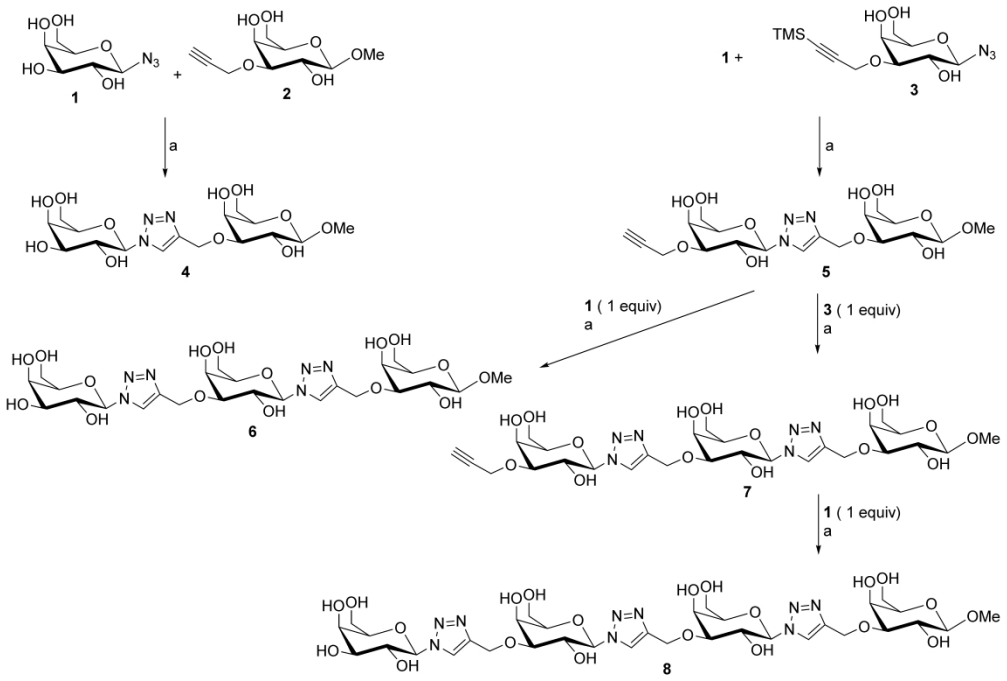

Scheme 1. Synthesis of mono-, di-, tri- and tetragalactosides. Reagent and conditions: a) CuSO4 (5 mol%), sodium ascorbate (10 mol%), o-phenylenediamine (15 mol%), H2O-tBuOH (1:1), RT, overnight.

272x184mm (600 x 600 DPI)

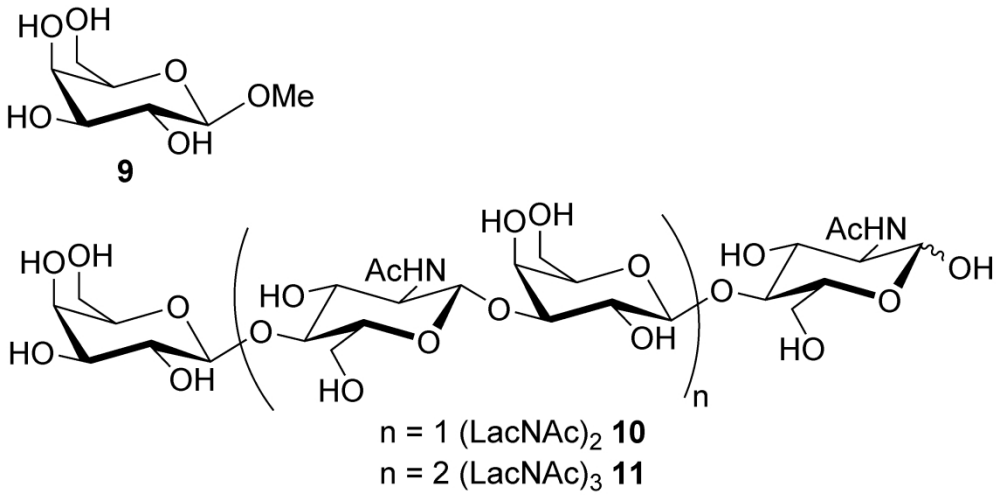

Figure 1. Reference compounds: Methyl β-D-galactopyranoside 9 and di- and tri-lactosamine 10 and 11

134x67mm (600 x 600 DPI)

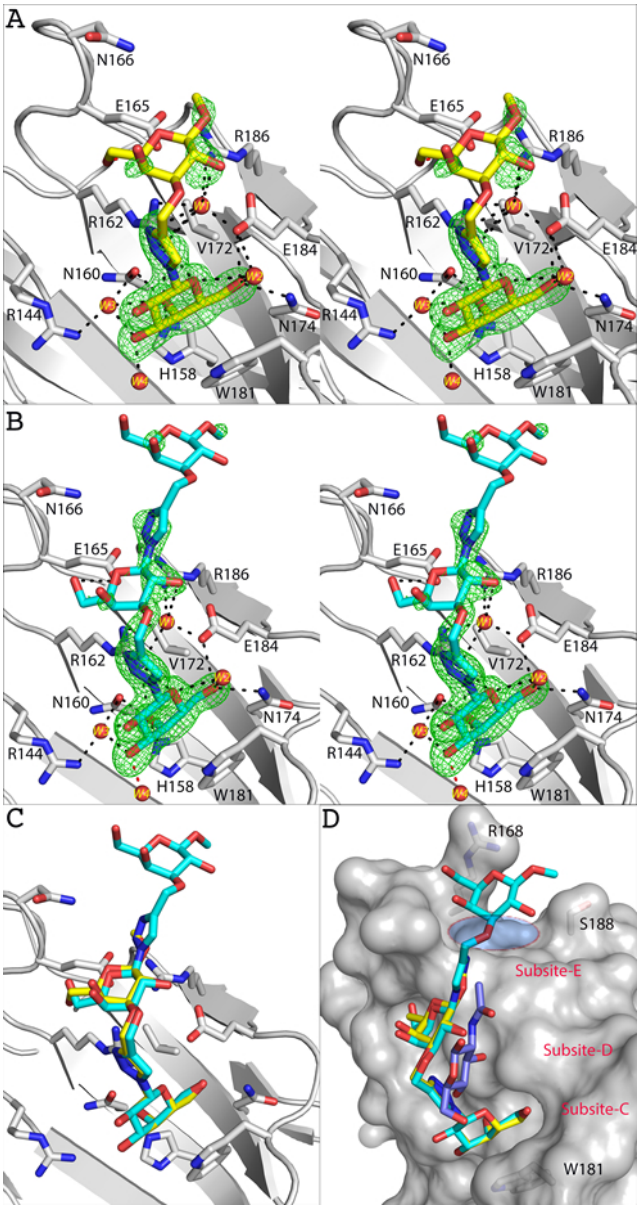

. A) Stereo diagram of the 2|Fo|-|Fc|αc map of compound 4 (at 1 σ) (yellow stick) (PDB ID 6Q17) bound within the galectin-3 CRD. Galectin-3 is depicted as a grey ribbon and interacting residues indicated as a grey sticks, hydrogen bonds indicated as a dashed black line. The water molecules interacting with compound 4 indicated as red spheres. B) Stereo diagram of the 2|Fo|-|Fc|of compound 6 (cyan stick) (PDB ID 6Q0Q) at 1 σ at CRD binding site of galectin-3. C) Alignment of the crystal structures of galectin-3 CRD in complex with 4 and 6 showing the upstream galactose and triazole rings could fit into the carbohydrate recognition site of the galectin-3 CRD whilst the downstream substituents adopt orientation toward subsite E. D) Comparison of compounds 4 and 6 with N-acetyllactosamine (LacNAc as a purple blue stick) (PDB ID:1KJL)[47] in CRD of galectin-3 to indicate that the 1-4 glycosidic of LacNac is more flexible and bend toward subsite D. The downstream galactose ring of compound 4 and the central galactose ring of compound 6 bend towards subsite E whilst the downstream galactose ring of compound 6 extends from subsite E and could approach the groove (red oval circle) between R168 and S188 for additional binding.

41x79mm (300 x 300 DPI)

A series of *pseudo* oligogalactosides as novel scaffold for galectin inhibitors obtained through iterative copper-catalyzed azide-alkyne cycloaddition is described. X-ray crystal structures of di- and tri-galactosides with galectin-3 reveal their orientation within the carbohydrate recognition domain (CRD) and suggest suitable modifications to develop novel inhibitors against this therapeutic target.

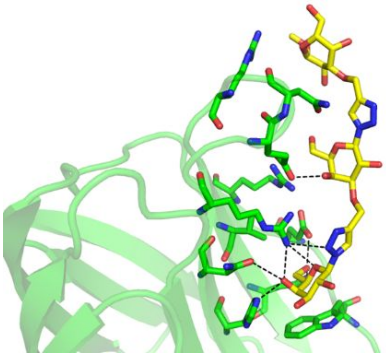

Linear triazole-linked *pseudo* oligogalactosides as scaffolds for galectin inhibitor development

Christophe Dussouy, Chandan Kishor, Annie Lambert, Clément Lamoureux, Helen Blanchard,* and Cyrille Grandjean*